

See discussions, stats, and author profiles for this publication at: <https://www.researchgate.net/publication/228535287>

Evidence for the Growth Mechanisms of Silver Nanocubes and Nanowires

ARTICLE *in* THE JOURNAL OF PHYSICAL CHEMISTRY C · MAY 2011

Impact Factor: 4.77 · DOI: 10.1021/jp2010088

CITATIONS

32

READS

70

5 AUTHORS, INCLUDING:



Sujie Chang

University of Science and Technology of China

15 PUBLICATIONS 277 CITATIONS

[SEE PROFILE](#)



Kai Chen

University of Science and Technology of China

8 PUBLICATIONS 223 CITATIONS

[SEE PROFILE](#)



Qing Hua

University of Science and Technology of China

22 PUBLICATIONS 503 CITATIONS

[SEE PROFILE](#)



Weixin Huang

University of Science and Technology of China

107 PUBLICATIONS 1,995 CITATIONS

[SEE PROFILE](#)

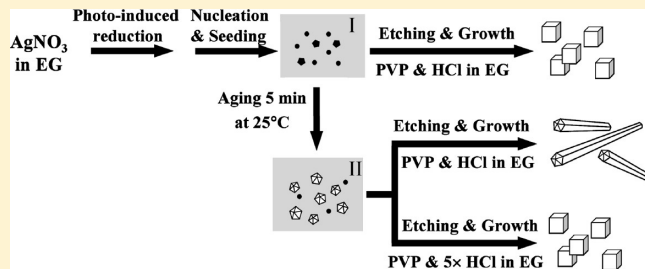
Evidence for the Growth Mechanisms of Silver Nanocubes and Nanowires

Sujie Chang,^{†,‡,§} Kai Chen,^{||} Qing Hua,^{†,‡,§} Yunsheng Ma,[§] and Weixin Huang^{*,†,‡,§}

[†]Hefei National Laboratory for Physical Sciences at the Microscale, [‡]CAS Key Laboratory of Materials for Energy Conversion, [§]Department of Chemical Physics, and ^{||}Education Center of Chemical Practice, University of Science and Technology of China, Hefei 230026, China

S Supporting Information

ABSTRACT: Ethylene glycol reduction of silver nitrate at 140 °C in the presence of poly(vinyl pyrrolidone) (PVP) and HCl is a facile method to prepare uniform silver nanocubes (Im et al., *Angew. Chem., Int. Ed.* 2005, 44, 2154). We reported herein that the product switches from uniform silver nanocubes to uniform silver nanowires by simply aging the freshly prepared AgNO₃ solution under ambient atmosphere for 5 min without the change of any other reaction parameters. The aging process was found to increase the density of silver seeds and, more importantly, to change the population of single and twinned crystal seeds. The portion of twinned-crystal seeds is less than 30% of total silver seeds in the freshly prepared AgNO₃ solution but more than 60% of total silver seeds in the AgNO₃ solution aged for 5 min. We proposed that twinned-crystal silver seeds in the freshly prepared AgNO₃ solution can be adequately etched in the subsequent etching and growth process, leading to the growth of silver nanocubes, but that those in the AgNO₃ solution aged for 5 min can not, leading to the growth of silver nanowires. Twinned-crystal silver seeds in the AgNO₃ solution aged for 5 min could be effectively etched by the increase of the concentration of HCl, yielding uniform silver nanocubes again. These results unambiguously prove the important role of twinned-crystal seeds in the growth of anisotropic silver metal nanowires and also indicate that the morphology of silver nanostructures prepared by the polyol process in the presence of PVP can be tuned by controlling the interplay between the population of twinned-crystal silver seeds and the concentration of HCl, greatly deepening the fundamental understanding of the growth mechanisms of silver nanocubes and nanowires.



1. INTRODUCTION

The shape of a metal nanocrystal determines the types of crystal planes exposed on its surface and thus greatly affects its properties and functions, particularly in catalysis and electrocatalysis exclusively occurring on the nanocrystal surface; therefore, tailoring the shape of nanocrystals is becoming an emerging strategy to innovate functional materials. The solution synthesis of shape-controlled metal nanocrystals has achieved great progress¹ since the early examples of Pt nanocubes and tetrahedrons,² Au nanorods,³ FePt nanocubes,⁴ Ag nanoplates,⁵ and Ag nanocubes.⁶ Meanwhile, great efforts have also been devoted to fundamentally understanding mechanisms controlling the shape evolution of a metal nanocrystal.^{1,7–9} When its growth occurs in an inert gas or vacuum, a fcc metal crystal assumes the so-called Wulff polyhedron as the equilibrium shape according to Wulff's construction.¹⁰ However, in a complex solution synthesis, the product often adopts a shape drastically different from the Wulff polyhedron. The growth of a metal nanocrystal during the solution synthesis can be divided into three stages: nucleation (reduction of metal ions to zerovalent atoms), seeding (evolution from nuclei to seeds), and growth (evolution from seeds to nanocrystals). By modifying the thermodynamics and kinetics at each stage of the

solution synthesis, shape-controlled metal nanocrystals can be synthesized. Successful approaches include the addition of seed particles to modify the nucleation and seeding processes, the selective oxidative etching to control the structure and population of seeds (single-crystal, singly twinned, and multiply twinned structures), and the selective chemisorption of capping agents to modify the surface free energy and growth rate of different crystal facets.¹

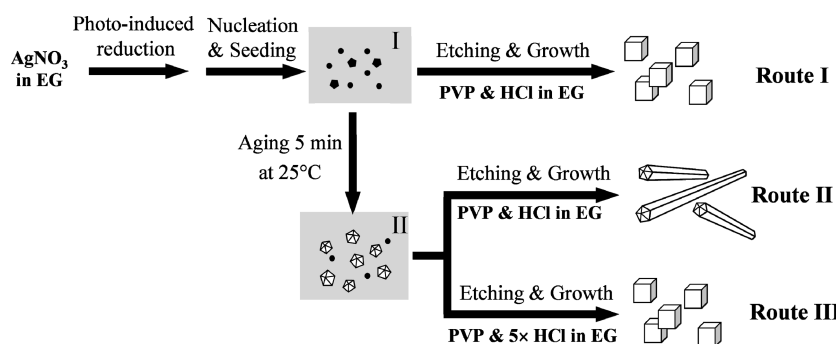
The comprehensive understanding of the underlying mechanism of the shape-controlled solution synthesis of metal nanocrystals will certainly advance the synthesis of metal nanocrystals with a designed shape but remains as a great challenge because of the complexity of solution synthesis. Suitable systems have to be developed to provide experimental evidence unambiguously and comprehensively demonstrating the role of different experimental parameters in the controlled shape evolution of a metal nanocrystal. Silver nanostructures with controlled shapes synthesized via the ethylene glycol (EG) reduction of silver nitrate at

Received: January 31, 2011

Revised: March 22, 2011

Published: April 04, 2011

Scheme 1. Schematic Illustration of Controllable Synthesis of Silver Nanocubes and Nanowires via the Ethylene Glycol Reduction of Silver Nitrate at 140 °C in the Presence of PVP and HCl



160 °C, which has been extensively investigated by Xia's group,¹¹ provide such a platform. Uniform silver nanowires were synthesized in the presence of poly(vinyl pyrrolidone) (PVP) employing Pt or Ag nanoparticles as seeds, but it is noteworthy that both silver nanowires and nanoparticles coexisted as the products.¹² By controlling the AgNO_3 concentration and the molar ratio between the repeating unit of PVP and AgNO_3 , silver nanocubes were successfully synthesized with a high yield.⁶ A likely growth mechanism for anisotropic silver nanowires was also proposed by Sun et al.:¹³ each silver nanowire evolved from a 5-fold twinned decahedral silver seed at the initial stage of the Ostwald ripening process, and the {100} facets were selectively covered by PVP but the {111} facets largely uncovered and thus highly reactive, resulting in the subsequent anisotropic growth. Among different seed structures (single-crystal, singly twinned, and multiply twinned structures), multiply twinned decahedra are the naturally abundant morphology^{10b} but are also the most reactive because of their twin defects.⁸ By selectively etching multiply twinned decahedral seeds by O_2/Cl^- (NaCl), silver nanocubes and cuboctahedra, instead of silver nanowires, were synthesized with a high yield via the same route;¹⁴ when Cl^- (NaCl) was substituted with Br^- (NaBr), seeds with a single twin plane could be selectively produced, leading to the synthesis of silver singly twinned right bipyramids.¹⁵ Furthermore, by introducing the Fe(II)-Fe(III) redox cycle to couple the O_2/Cl^- oxidative etching reaction, the morphology of silver nanostructures could be controlled with a high yield either in nanocubes or in nanowires.¹⁶ In these reported systems, uniform silver nanostructures with various shapes were successfully prepared employing the same strategy at the same reaction temperature, which nicely demonstrates the important role of seed structures and selective etching processes in the shape evolution of metal nanocrystals; however, important reaction parameters such as the types and concentrations of reactants differed among synthesis routes for different silver nanostructures, which to some extent hinders the understanding of relevant fundamental issues.

Im et al.¹⁷ reported the synthesis of monodispersed silver nanocubes via the EG reduction of silver nitrate at 140 °C in the presence of PVP and HCl (Route I in Scheme 1), in which the selective etching and dissolution of twinned-crystal silver seeds was proposed to play the key role. In this paper, we report an interesting finding that this synthesis route for silver nanocubes can be modified to synthesize silver nanowires at a very high yield only by aging the fresh AgNO_3 solution under ambient atmosphere without the change of any other reaction parameters (Route II in Scheme 1).

We found that the structure and population of silver seeds formed in the AgNO_3 solution evolve during the aging process in which the quantity of twinned-crystal silver seeds is too large to be etched away, leading to the synthesis of silver nanowires with a very high yield. This simple but beautiful system provides direct and unambiguous experimental evidence for the important role of seed crystal structures and etching processes in the shape-controlled solution synthesis of silver nanostructures. The large quantity of twinned-crystal silver seeds formed during the aging process could be etched away by increasing the concentration of HCl, leading to the synthesis of silver nanocubes again (Route III in Scheme 1). This observation clearly demonstrates the contribution of HCl to the selective etching and dissolution of twinned silver seeds in this synthesis route. Our results also point out a reliable way to control the morphology of silver nanostructures in this synthesis by controlling the interplay between the population of twinned-crystal silver seeds and the concentration of HCl. The fundamental understanding might be extended to other solution synthesis systems of shape-controlled fcc metal nanostructures.

2. EXPERIMENTAL SECTION

2.1. Synthesis of Silver Nanostructures. All chemicals including AgNO_3 ($\geq 99.8\%$), EG ($\geq 99.0\%$, the chloride content $\leq 0.005\%$), PVP (K-30), and HCl (36.0–38.0%) were purchased from Sinopharm Chemical Reagent Co., Ltd. and used as received without further purification. Without specifications, experiments were conducted under ambient atmosphere (room temperature: 25 °C). Silver nanocubes were synthesized using the polyol method described in ref 17. In a typical synthesis, 25 mL of EG was placed in a 100 mL three-necked flask, capped and heated with stirring in an oil bath at 140 °C for 1 h. An amount of 5 mL of HCl solution (25 μM in EG) was then quickly added, and the vial was recapped. After 10 min, 15 mL of freshly prepared AgNO_3 solution (94 mM in EG, and the dissolution process took about 5 min using ultrasonic baths) and 15 mL of PVP solution (147 mM in EG in terms of the repeating unit) were simultaneously injected with a two-channel syringe pump at a rate of 45 mL/h to the stirring solution. The vial was then recapped and heated at 140 °C. The reaction was stopped after 8 h, and the suspending solid was isolated by centrifugation at 11 000 rpm and then washed with ethanol and water to remove excess EG and PVP prior to structural characterizations. Silver nanowires were synthesized under the same conditions except for the aging of the freshly prepared AgNO_3 solution for 5 min

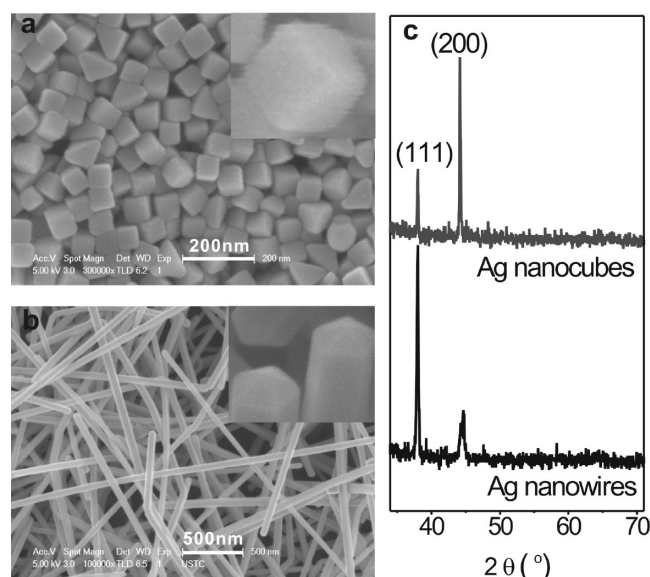


Figure 1. SEM images of silver nanocubes (a) and nanowires (b) and the corresponding XRD patterns (c). The insets are amplified images.

under ambient atmosphere prior to its injection, and the reaction lasted 90 min after the injection. For the purpose of comparison, EG with a very low chloride content (<1 ppm) purchased from Mallinckrodt Baker, Inc. (denoted as J. T. Baker EG) was also used for the synthesis of silver nanocrystals.

2.2. Structural Characterizations. UV-vis absorption spectra were recorded on a Shimadzu UV-2450 spectrophotometer at room temperature using EG as the reference solution. Scanning electron microscopy (SEM) images were taken using a field emission scanning electron microscope (FEI, Sirion200). Transmission electron microscopy (TEM) and high-resolution transmission electron microscopy (HRTEM) images were obtained using JEOL-2010 microscope operating at 200 kV. Specimens for TEM and HRTEM analysis were prepared by fishing silver nanocrystals in the sample solution using holey-carbon-coated copper grids followed by drying in a vacuum oven. Powder X-ray diffraction (XRD) patterns were performed on a Philips X'Pert PROS diffractometer using a Cu K α (wavelength: 0.154 18 nm) radiation source. For an XRD measurement, silver nanocrystals were ultrasonically dispersed in ethanol and dropped on a glass plate.

3. RESULTS AND DISCUSSION

Figure 1a shows the SEM image of synthesized silver nanocubes. The synthesized silver nanocubes reproduce quite well those reported in ref 17, being uniform with edge lengths between 70 and 80 nm. Interestingly, the product switches from uniform silver nanocubes to uniform silver nanowires (Figure 1b) by the same synthesis route with the same reaction conditions except for the aging of the freshly prepared AgNO₃ solution for 5 min under ambient atmosphere prior to its injection. The average diameter of silver nanowires is ~40 nm, and their lengths vary between 3 and 12 μ m. It can be clearly seen that from the inset in Figure 1b that the silver nanowires have 5-fold symmetry, agreeing with silver nanowires reported in the literature.^{12,16} Few silver nanoparticles were observed in the product separated by centrifugation at 11 000 rpm, indicating a very high yield of silver nanowires. Figure 1c presents the XRD patterns of silver nanocubes and nanowires. Only the

(111) and (200) diffraction peaks were observed, but the (220) diffraction peak was not, verifying the homogeneity of our silver nanostructures. The peak intensity ratio of (200)/(111) for silver nanocubes (2.36) is much higher than that of silver nanowires (0.6), implying that silver nanocubes were assembled more regularly on the glass substrate than silver nanowires during the specimen preparation process.

The growth process of silver nanowires and nanocubes after the injection of AgNO₃ solution was investigated in detail by UV-vis absorption spectra and SEM. The finish of the injection was set as 0 min. Figure 2 shows the UV-vis spectra at different growth stages of silver nanocubes, photographs of corresponding reaction solutions, and SEM images of corresponding silver nanostructures. The color of the reaction solution changes at different stages. At 0 min, the solution is translucent yellow, and the UV-vis absorption spectrum displays a peak at 407 nm that is normally attributed to in-plane dipole surface plasmon resonance (SPR) of silver nanoparticles. The solution is still yellow but a little lighter after 40 min reaction. The corresponding UV-vis absorption peak locates at 415 nm, indicating the growth in the size of silver nanoparticles.¹⁸ The corresponding SEM image (Figure 2b) demonstrates the formation of spherical silver nanoparticles with diameters between 40 and 50 nm at this growth stage. With the further proceeding of the reaction, the solution fades in color and becomes almost colorless after 3 h. The corresponding UV-vis absorption spectrum does not show any obvious peaks. However, we found that the Tyndall phenomenon could still be clearly observed for this reaction solution, demonstrating the existence of silver colloids. Such a similar colorless reaction solution was also observed previously by Im et al.,¹⁷ which suggests the complete dissolution of all large silver nanoparticles. Then the color of the solution gradually becomes dark and is translucent yellow after 5 h reaction. The corresponding UV-vis absorption peak locates at 429 nm, and the corresponding SEM image (Figure 2c) demonstrates the formation of silver nanoparticles with irregular morphologies and a wide size range between 30 and 220 nm. The reaction solution turns opaque as the reaction continues. When the reaction was stopped at 8 h, the solution was khaki slurry. After being diluted with EG 3×10^4 times, the solution shows a broad peak centering at 452 nm in the UV-vis absorption spectrum. The corresponding SEM image (Figure 2d) proves the production of uniform silver nanocubes with their edge lengths of 70–80 nm.

Figure 3 shows the UV-vis spectra at different growth stages of silver nanowires, photographs of corresponding reaction solutions, and SEM images of corresponding silver nanostructures. The color of the reaction solution changes from yellow to gray but does not experience the coreless stage. After 10 min reaction, the UV-vis absorption peak of the reaction solution shifts from 413 to 440 nm, suggesting a growth in the particle size. The product at 10 min (Figure 3b) includes both spherical and rodlike silver nanoparticles. After another 10 min reaction, the product (Figure 3c) mainly consists of silver nanowires with lengths of 1–5 μ m and diameters of 30–50 nm. Two peaks at 356 and 385 nm develop at the expense of that at 440 nm in the corresponding UV-vis absorption spectrum. Both peaks at 356 and 385 nm could be reasonably assigned to SPR of silver nanowires and that at 440 nm to SPR of silver nanoparticles. After 30 min reaction, the UV-vis spectrum shows very strong absorption peaks at 356 and 385 nm but no peak at 440 nm; accordingly, the SEM image (Figure 3d) proves the growth of uniform silver nanowires.

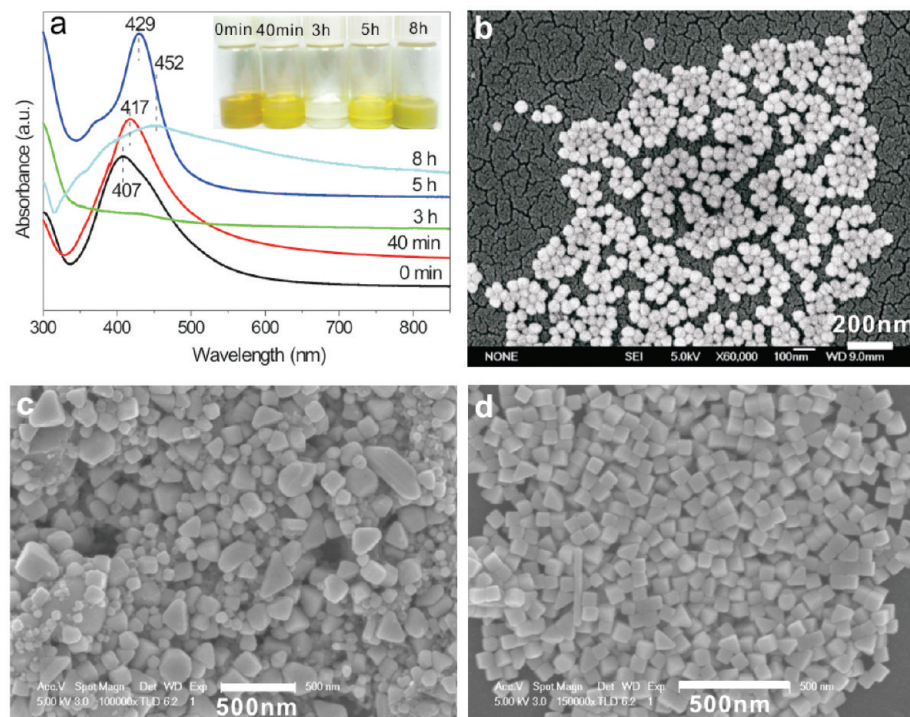


Figure 2. UV-vis absorption spectra (a) of the reaction mixture for the synthesis of silver nanocubes at indicated reaction times and SEM images of silver nanostructures at different reaction times (b, 40 min; c, 5 h; d, 8 h). The inset shows the photographs of the reaction mixture at indicated reaction times.

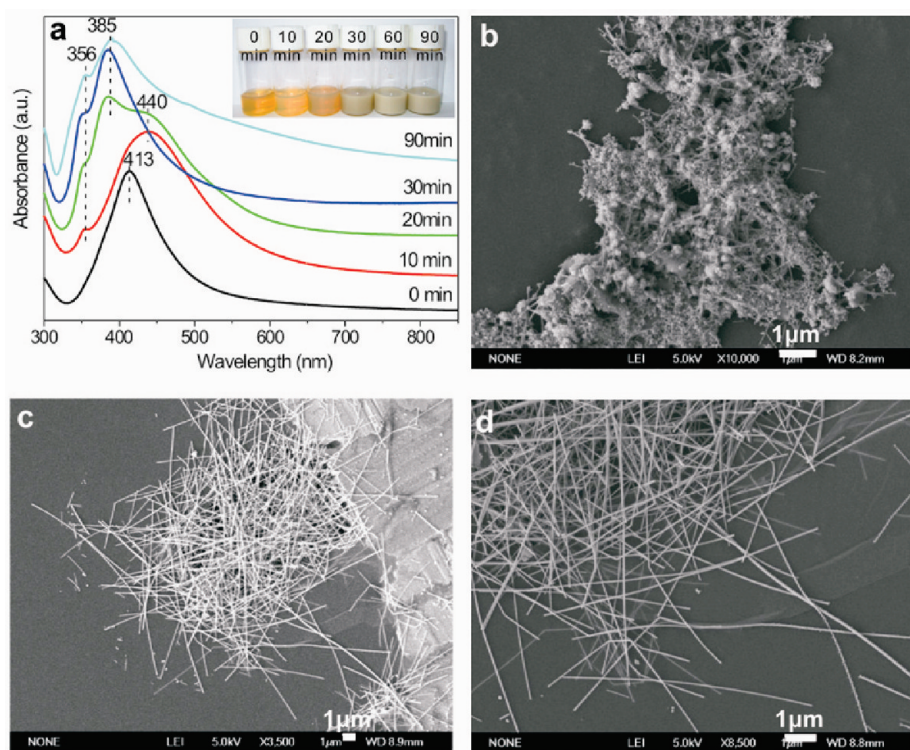


Figure 3. UV-vis absorption spectra (a) of the reaction mixture for the synthesis of silver nanowires at indicated reaction times and SEM images of silver nanostructures at different reaction times (b, 10 min; c, 20 min; d, 30 min). The inset shows the photographs of the reaction mixture at indicated reaction times.

The above results clearly show that the product switches from uniform silver nanocubes to uniform silver nanowires in

the EG reduction of silver nitrate by aging of the freshly prepared AgNO_3 solution for 5 min under ambient atmosphere

without the change of any other reaction parameters. The aging process of the freshly prepared AgNO_3 solution was then studied in detail. Figure 4 shows UV-vis absorption spectra of the freshly prepared AgNO_3 solution and AgNO_3 solutions aged for 5 and 10 min and corresponding photographs. The freshly prepared AgNO_3 solution is transparent light yellow and then becomes brown and dark brown after the solution is aged for 5 and 10 min, respectively. The UV-vis absorption spectrum of the freshly prepared AgNO_3 solution displays a broad peak centering at 428 nm. The peak shifts to 442 and 447 nm after aging for 5 and 10 min, respectively; meanwhile, the peak intensity also grows with the aging time. These results demonstrate that the reduction of AgNO_3 by EG occurs during its dissolution in EG under ambient atmosphere, leading to the formation of silver nuclei and seeds, and the aging of the freshly prepared AgNO_3 solution increases the density of silver nuclei and seeds.

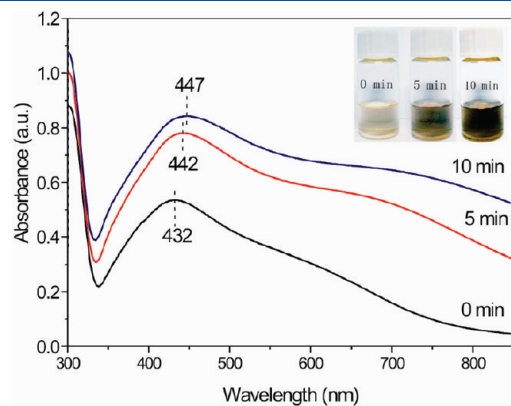


Figure 4. UV-vis absorption spectrum of the AgNO_3 solution dissolved in EG aged for various times. The inset shows the corresponding photographs.

The structure of silver seeds in the freshly prepared AgNO_3 solution and the AgNO_3 solution aged for 5 min was further studied with TEM and HRTEM. Figures 5a and 5c show the representative TEM and HRTEM images of silver seeds in the freshly prepared AgNO_3 solution, respectively. The silver seeds consist of single and twinned crystals whose population and size distribution were counted and shown in Figure 5e. In the freshly prepared AgNO_3 solution, more than 70% silver seeds are fine single crystals. The remaining are twinned crystals whose sizes are much larger than those of single crystals. As shown in Figures 5b, 5d, and 5f, after aging for 5 min, the silver seeds still consist of single and twinned crystals whose sizes are similar to those in the freshly prepared AgNO_3 solution; however, the population of single and twinned crystals changes greatly. The proportion of twinned crystals increases to above 60%.

On the basis of the UV-vis absorption spectra and TEM results, it can be inferred that silver seeds formed by the EG reduction of AgNO_3 during the dissolution process mainly are fine single crystals. During the following aging process, the density of silver nuclei and seeds increases, and more importantly, twinned-crystal seeds form at the expense of single-crystal seeds and compose the majority of silver seeds. This is reasonable because multiply twinned crystals are the most thermodynamically stable seeds.^{10b} The silver seeds with different populations of single crystals and twinned crystals undergo different evolution pathways under the same reaction conditions. We investigated silver nanostructures formed as soon as the AgNO_3 solutions were injected into EG in the presence of HCl at 140 °C using TEM and HRTEM. For the freshly prepared AgNO_3 solution (Figure 6a and 6b), fine spherical nanoparticles with a diameter between 2 and 5 nm and a few large ones (~ 20 nm) were observed, and importantly, almost all of them are single crystals. This indicates that the large twinned-crystal silver seeds have been etched and dissolved during the injection process, and fine silver seeds mostly with the single-crystal structure have reformed. Among seeds with single crystal, singly

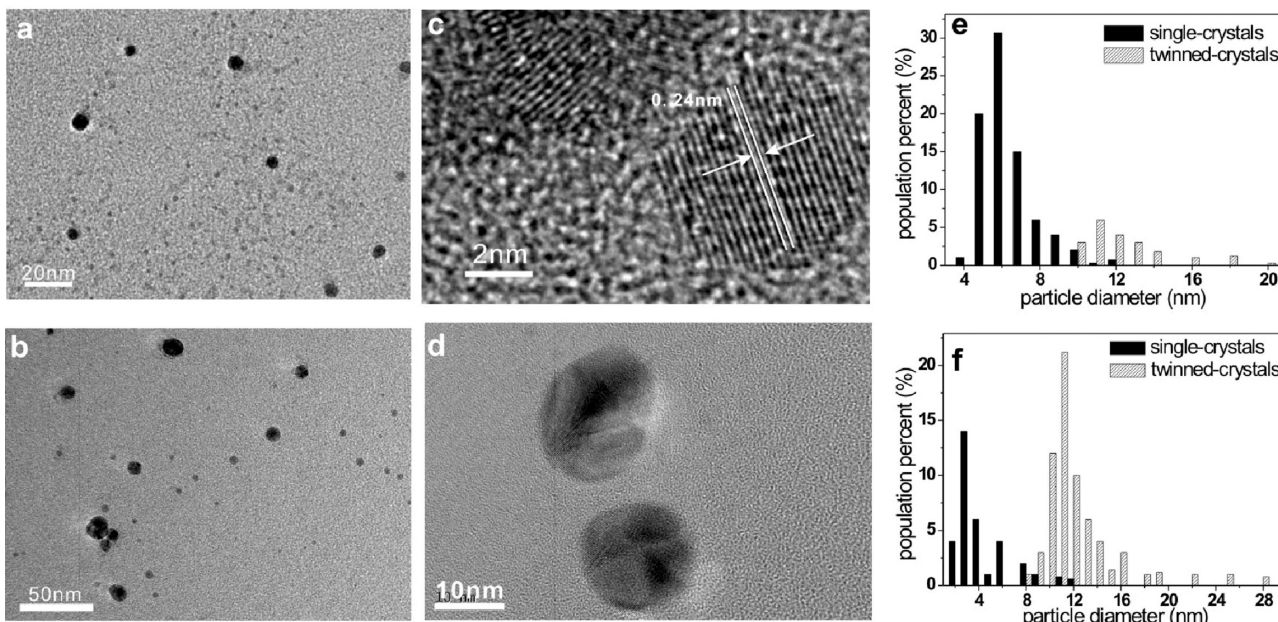


Figure 5. TEM (a) and HRTEM (c) images and the size distribution and population (e) of silver seeds formed as soon as AgNO_3 was dissolved in EG; and TEM (b) and HRTEM (d) images and the size distribution and population (f) of silver seeds formed after the AgNO_3 solution dissolved in EG was aged for 5 min.

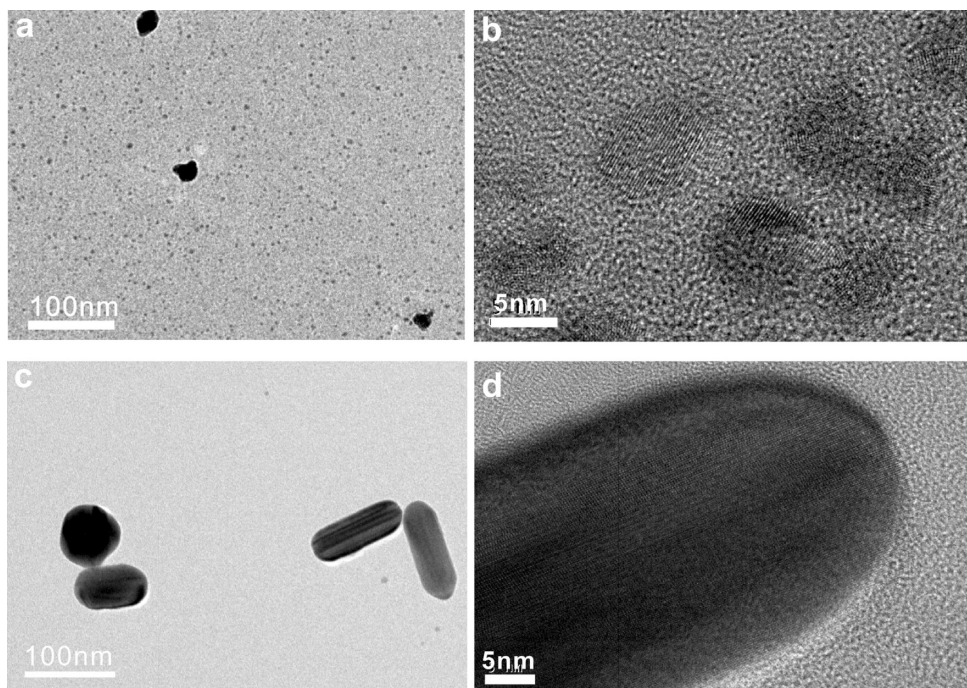


Figure 6. TEM and HRTEM images of silver nanoparticles formed as soon as the AgNO_3 in EG solution without aging (a and b) and aged for 5 min (c and d) was injected simultaneously with the PVP in EG solution into the EG solution containing HCl.

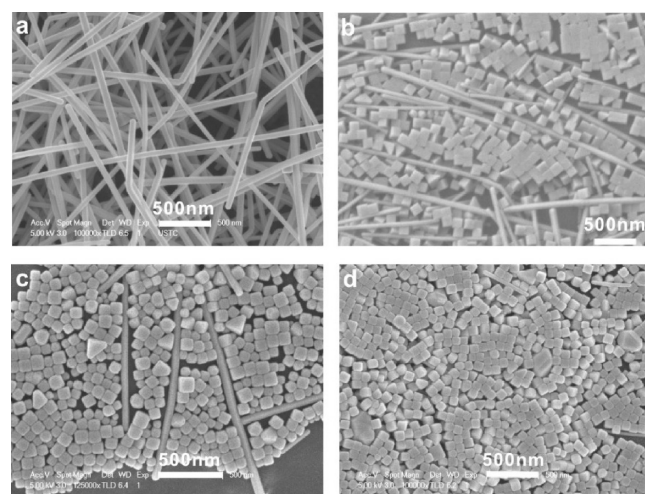


Figure 7. SEM images of final silver nanostructures synthesized with different HCl concentrations: (a) $25 \mu\text{M}$; (b) $50 \mu\text{M}$; (c) $75 \mu\text{M}$; (d) $125 \mu\text{M}$.

twinned, and multiply twinned structures, multiply twinned crystal seeds are most reactive because of their twin defects.⁸ Two different types of etchants were proposed to exist in this system: HNO_3 and O_2/Cl^- .^{14,17,19} For the AgNO_3 solution aged for 5 min (Figure 6c and 6d), however, some large twinned-crystal silver seeds survive under the same reaction conditions and mainly evolve into nanorods ($\sim 100 \text{ nm}$ in length and $\sim 30 \text{ nm}$ in diameter) together with a few spherical nanoparticles, most of which are with the multiply twinned structure. We believed that the concentrations of etchants (HNO_3 and O_2/Cl^-) governed by the HCl concentration employed in the synthesis ($25 \mu\text{M}$) were too low to adequately etch and dissolve

the large population of twinned-crystal silver seeds in the AgNO_3 solution aged for 5 min. This argument is supported by experimental results of the same synthesis systems employing the AgNO_3 solution aged for 5 min except the HCl concentration. The SEM results (Figure 7) clearly demonstrate that the morphology of silver nanocrystals gradually changes from nanowires to nanocubes with the increase of the employed HCl concentration. When the HCl concentration reached $125 \mu\text{M}$, uniform silver nanocubes were synthesized again with a high yield. This observation unambiguously proves the HCl concentration as an important factor in the selective etching and dissolution of twinned-crystal silver seeds.

The reducing ability of EG is weak at room temperature and strengthens at elevated temperatures,^{11,20} however, the photoinduced reduction of silver salts including AgCl is well known to occur at room temperature,^{5,21} and Cl^- is a common type of impurity in EG. To clarify the formation and evolution mechanism of silver seeds during the dissolution and subsequent aging process of AgNO_3 in EG at room temperature, the following controlled experiments were conducted. The first is to employ AgNO_3 solution whose preparation and aging were conducted in the dark at room temperature for the synthesis while other reaction parameters remained unchanged. The UV-vis spectra (Supporting Information, Figure S1a) clearly demonstrate that the freshly prepared AgNO_3 solution contains few silver seeds, and aging the freshly prepared AgNO_3 solution in the dark at room temperature does not result in any obvious changes, indicating that the formation of silver seeds during the dissolution of AgNO_3 in EG at room temperature must be a photoinduced reduction process. Reasonably uniform silver nanocubes were the only product (Supporting Information, Figures S1b and S1c) no matter which AgNO_3 solution was employed.

The second controlled experiment is to replace the employed Sinopharm EG (chloride content $\leq 0.005\%$) with J. T. Baker EG (chloride content $< 1 \text{ ppm}$) in the preparation of AgNO_3 solution

while other reaction parameters did not change. The UV-vis spectra (Supporting Information, Figure S2a) show that the freshly prepared AgNO_3 solution contains few silver seeds, but the aging process does lead to the increase of the density of silver seeds. However, compared with Figure 4, it can be inferred that the density of silver seeds employing J. T. Baker EG is much less than that employing Sinopharm EG, indicating that the presence of Cl^- also facilitates the photoinduced reduction of AgNO_3 in EG at room temperature. Uniform silver nanocubes are the only product starting from the freshly prepared AgNO_3 solution (Supporting Information, Figure S2b), and silver nanowires and nanocubes coexist in the product starting from the AgNO_3 solution aged for 5 min (Supporting Information, Figure S2c), which should be related with the density and population of single-crystal and twinned-crystal silver seeds in the starting AgNO_3 solution.

Therefore, the above controlled experiments demonstrate that the photoinduced reduction of AgNO_3 in the presence of Cl^- is responsible for the formation and evolution of silver seeds during the dissolution and subsequent aging process of AgNO_3 in EG at room temperature; however, the resulting different types of silver seeds turn out to offer suitable and nice platforms to manifest the important role of seed structures in their subsequent growth. Scheme 1 summarizes our main findings. As previously reported by Im et al.,¹⁷ Route I in Scheme 1 is a convenient method to synthesize uniform silver nanocubes with a high yield. We found that the synthesized product becomes uniform silver nanowires with a high yield by aging of the freshly prepared AgNO_3 solution for 5 min under ambient atmosphere without the change of any other reaction parameters (Route II in Scheme 1). Therefore, Route I and Route II compose a suitable model system to fundamentally understand factors controlling the morphology of silver nanocrystals prepared by the polyol process in the presence of PVP. Our results reveal that the structure and population of silver seeds formed in the AgNO_3 solution play an important role in the morphology of synthesized silver nanocrystals. Both silver seeds formed in the freshly prepared AgNO_3 solution of route I (Type I) and those in the AgNO_3 solution aged for 5 min of route II (Type II) consist of single crystals and twinned crystals. The size distribution of single-crystal and twinned-crystal silver seeds in both types is similar; however, the population of single-crystal and twinned-crystal silver seeds differs greatly in Type I and Type II silver seeds. The portion of single-crystal silver seeds is more than 70% in Type I, whereas that of twinned-crystal silver seeds is more than 60% in Type II. Moreover, the density of Type II silver seeds is much larger than that of Type I silver seeds. Under the same reaction conditions, twinned-crystal seeds in Type I silver seeds can be adequately etched, and thus uniform silver nanocubes are synthesized; however, twinned-crystal seeds in Type II silver seeds can not, and thus uniform silver nanowires are obtained. However, twinned-crystal seeds in Type II silver seeds can be effectively etched by increasing the HCl concentration, and thus the concentration of etchants in the reaction system (Route III in Scheme 1) and uniform silver nanocubes are acquired again. These results provide solid experimental evidence for the growth mechanism in the polyol process proposed previously^{8,9,13} that anisotropic silver nanowires evolve from twinned-crystal seeds in the presence of PVP. These results also demonstrate that uniform silver nanocubes can be prepared with a high yield in the polyol process as long as twinned-crystal seeds formed during the dissolution of AgNO_3 in EG can be adequately etched. Therefore, the morphology of silver nanostructures prepared by the polyol process in the presence of

PVP can be tuned by controlling the interplay between the population of twinned-crystal silver seeds and the concentration of etchants. This finding will greatly facilitate the reproducible preparation of uniform silver nanostructures. Since the solution synthesis of fcc metal nanostructures all involves nucleation, seeding, and growth, we believe that our findings reported herein might be extended to other solution synthesis systems of shape-controlled fcc metal nanostructures.

4. CONCLUSIONS

We have successfully provided solid experimental evidence for the fundamental understanding of the growth mechanisms of silver nanocubes and nanowires prepared via the EG reduction of silver nitrate at 140 °C in the presence of PVP and HCl. The photoinduced reduction of AgNO_3 in the presence of Cl^- can result in the formation and structural evolution of silver seeds during the dissolution and subsequent aging process of AgNO_3 in EG at room temperature. Aging the freshly prepared AgNO_3 solution under ambient atmosphere for 5 min without the change of any other reaction parameters can switch the silver nanostructures from uniform nanocubes to uniform nanowires. The aging process increases the density of silver seeds and, more importantly, changes the population of single-crystal seeds and twinned-crystal seeds in silver seeds. The portion of twinned-crystal seeds is less than 30% in silver seeds in the freshly prepared AgNO_3 solution and can be adequately etched during the following process, leading to the preparation of uniform silver nanocubes; however, the portion of twinned-crystal seeds increases to more than 60% in silver seeds in the AgNO_3 solution aged for 5 min and thus can not be effectively etched, leading to the synthesis of uniform silver nanowires under the same reaction conditions. These results directly and unambiguously prove the important role of seed crystal structures and etching processes in the shape-controlled solution synthesis of silver nanostructures. Increasing the concentration of HCl and thus the concentration of etchants can effectively etch a large quantity of twinned-crystal silver seeds in the AgNO_3 solution aged for 5 min and then yield uniform silver nanocubes again. These results indicate that the morphology of silver nanostructures prepared by the polyol process in the presence of PVP can be tuned by controlling the interplay between the population of twinned-crystal silver seeds and the concentration of etchants, which will greatly facilitate the reproducible preparation of uniform silver nanostructures.

■ ASSOCIATED CONTENT

S Supporting Information. Figures S1 and S2. This material is available free of charge via the Internet at <http://pubs.acs.org>.

■ AUTHOR INFORMATION

Corresponding Author

*Fax: + 86-551-3600437. E-mail: huangwx@ustc.edu.cn.

■ ACKNOWLEDGMENT

This work was financially supported by the National Natural Science Foundation of China (grants 20773113), National Basic Research Program of China (2010CB923302), the Fundamental Research Funds for the Central Universities, and the MPG-CAS partner group program.

■ REFERENCES

- (1) Xia, Y.; Xiong, Y.; Lim, B.; Skrabalak, S. E. *Angew. Chem., Int. Ed.* **2009**, *48*, 60.
- (2) Ahmadi, T. S.; Wang, Z. L.; Green, T. C.; Henglein, A.; El-Sayed, M. A. *Science* **1996**, *272*, 1924.
- (3) Yu, Y.-Y.; Chang, S.-S.; Lee, C.-L.; Wang, C. R. C. *J. Phys. Chem. B* **1997**, *101*, 6661.
- (4) Sun, S.; Murray, C. B.; Weller, D.; Folks, L.; Moser, A. *Science* **2000**, *287*, 1989.
- (5) Jin, R.; Cao, Y.; Mirkin, C. A.; Kelly, K. L.; Schatz, G. C.; Zheng, J. G. *Science* **2001**, *294*, 1901.
- (6) Sun, Y.; Xia, Y. *Science* **2002**, *298*, 2176.
- (7) Murphy, C.; Sau, T.; Gole, A.; Orendorff, C. *Mater. Res. Bull.* **2005**, *30*, 349.
- (8) Lofton, C.; Sigmund, W. *Adv. Funct. Mater.* **2005**, *15*, 1197.
- (9) Elechiguerra, J. L.; Reyes-Gasga, J.; Yacaman, M. J. *J. Mater. Chem.* **2006**, *16*, 3906.
- (10) (a) Wulff, G. Z. *Kristallogr.* **1901**, *34*, 449. (b) Marks, L. D. *Rep. Prog. Phys.* **1994**, *57*, 603.
- (11) Wiley, B.; Sun, Y.; Xia, Y. *Acc. Chem. Res.* **2007**, *40*, 1067.
- (12) (a) Sun, Y.; Gates, B.; Mayers, B.; Xia, Y. *Nano Lett.* **2002**, *2*, 165. (b) Sun, Y.; Xia, Y. *Adv. Mater.* **2002**, *14*, 833. (c) Sun, Y.; Yin, Y.; Mayers, B. T.; Herricks, T.; Xia, Y. *Chem. Mater.* **2002**, *14*, 4736.
- (13) Sun, Y.; Mayers, B.; Herricks, T.; Xia, Y. *Nano Lett.* **2003**, *3*, 955.
- (14) Wiley, B.; Herricks, T.; Sun, Y.; Xia, Y. *Nano Lett.* **2004**, *4*, 1733.
- (15) Wiley, B.; Xiong, Y.; Li, Z.-Y.; Xia, Y. *Nano Lett.* **2006**, *6*, 765.
- (16) Wiley, B.; Sun, Y.; Xia, Y. *Langmuir* **2005**, *21*, 8077.
- (17) Im, S. H.; Lee, Y. T.; Wiley, B.; Xia, Y. *Angew. Chem., Int. Ed.* **2005**, *44*, 2154.
- (18) Sosa, I. O.; Noguez, C.; Barrera, R. G. *J. Phys. Chem. B* **2003**, *107*, 6269.
- (19) (a) Tang, X.-L.; Tsuji, M.; Jiang, P.; Nishio, M.; Jang, S.; Yoon, S.-H. *Colloids Surf., A* **2009**, *338*, 33. (b) Tang, X.-L.; Tsuji, M.; Nishio, M.; Jiang, P. *Bull. Chem. Soc. Jpn.* **2009**, *82*, 1304.
- (20) (a) Bock, C.; Paquet, C.; Couillard, M.; Botton, G. A.; MacDougall, B. R. *J. Am. Chem. Soc.* **2004**, *126*, 8028. (b) Liu, N.; Yin, L.; Wang, C.; Zhang, L.; Lun, N.; Wang, C.; Qi, Y. *J. Phys. Chem. C* **2010**, *114*, 22012.
- (21) (a) Henglein, A. *Langmuir* **2001**, *17*, 2329. (b) Qiu, L.; Franc, J.; Rewari, A.; Blanc, D.; Saravatamuttu, K. *J. Mater. Chem.* **2009**, *19*, 373. (c) Wang, P.; Huang, B.; Xin, Q.; Zhang, X.; Dai, Y.; Wei, J.; Whangbo, M.-H. *Angew. Chem., Int. Ed.* **2008**, *47*, 7931.